Bone 181 (2024) 117047

Contents lists available at ScienceDirect

Bone

journal homepage: www.elsevier.com/locate/bone

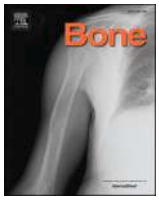

Full Length Article

A pathogenic role for brain-derived neurotrophic factor (BDNF) in fibrous dysplasia of bone

Biagio Palmisano [a,1], Giorgia Farinacci [a], Federica Campolo [b], Chiara Tavanti [a], Alessia Stefano [a], Samantha Donsante [a,2], Ernesto Ippolito [c], Giuseppe Giannicola [d], Mary Anna Venneri [b], Alessandro Corsi [a], Mara Riminucci [a,*]

[a] Department of Molecular Medicine, Sapienza University of Rome, 00161 Rome, Italy
[b] Department of Experimental Medicine, Sapienza University of Rome, 00161 Rome, Italy
[c] Department of Orthopaedic Surgery, University of Rome Tor Vergata, 00133 Rome, Italy
[d] Department of Anatomical, Histological, Medico Legal and Orthopaedic Sciences, Sapienza University of Rome, 00161 Rome, Italy

ARTICLE INFO

Keywords:
McCune Albright syndrome
Bone remodeling
Bone resorption
Osteoclastogenesis
Osteolysis
Osteogenesis
Bone fibrosis
Biopsy
Animal models

ABSTRACT

Brain derived neurotrophic factor (BDNF) is a neurotrophin, expressed in the central nervous system and in peripheral tissues, that is regulated by the Gsα/cAMP pathway. In bone, it regulates osteogenesis and stimulates RANKL secretion and osteoclast formation in osteolytic tumors such as Multiple Myeloma. Fibrous dysplasia (FD) of bone is a rare genetic disease of the skeleton caused by gain-of-function mutations of the Gsα gene in which RANKL-dependent enhanced bone resorption is a major cause of bone fragility and clinical morbidity.

We observed that BDNF transcripts are expressed in human FD lesions. Specifically, immunolocalization studies performed on biopsies obtained from FD patients revealed the expression of BDNF in osteoblasts and, to a lower extent, in the spindle-shaped cells within the fibrous tissue. Therefore, we hypothesized that BDNF can play a role in the pathogenesis of FD by stimulating RANKL secretion and bone resorption. To test this hypothesis, we used the EF1α-Gsα^{R201C} mouse model of the human disease (FD mice). Western blot analysis revealed a higher expression of BDNF in bone segments of FD mice compared to WT mice and the immunolabeling pattern within mouse FD lesions was similar to that observed in human FD. Treatment of FD mice with a monoclonal antibody against BDNF reduced the fibrous tissue along with the number of osteoclasts and osteoblasts within femoral lesions.

These results reveal BDNF as a new player in the pathogenesis of FD and a potential molecular mechanism by which osteoclastogenesis may be nourished within FD bone lesions. They also suggest that BDNF inhibition may be a new approach to reduce abnormal bone remodeling in FD.

1. Introduction

Brain derived neurotrophic factor (BDNF) is a neurotrophin that plays a key role in promoting neuronal development and survival [1,2]. It is produced by afferent sensory neurons and acts as a peripheral mediator and a central sensitizer of pain, and as a promoter of acute to chronic pain transition [2]. Like other members of the neurotrophin family, BDNF and its cognate tropomycin receptor kinase B (TRKB) [3], are also expressed in a wide range of non-nervous tissues and organs including endothelium, epithelium, hematopoietic marrow, skeletal muscle, spleen and liver in which they participate in the regulation of the differentiation and function of multiple types of target cells [4–9]. In the skeleton, BDNF is synthetized by osteogenic cells at all differentiation stages, from stromal progenitors to osteoblasts [10,11] and many studies demonstrate that it positively regulates bone formation and fracture healing [12–14]. In addition, recent evidence demonstrates that BDNF also acts as a promoter of osteoclastogenesis and that this function may be critical to the pathogenesis of lytic lesions associated with some neoplastic diseases. Specifically, in Multiple Myeloma [15–17] and bone metastasis of gastric cancer [18], BDNF produced by the tumor

* Corresponding author.
E-mail address: mara.riminucci@uniroma1.it (M. Riminucci).
[1] Present address: Department of Radiological, Oncological and Anatomo-pathological Science, Sapienza University of Rome, 00161 Rome, Italy.
[2] Present address: Tettamanti Center, Fondazione IRCCS San Gerardo dei Tintori, 20900 Monza, Italy.

https://doi.org/10.1016/j.bone.2024.117047
Received 6 December 2023; Received in revised form 10 January 2024; Accepted 6 February 2024
Available online 7 February 2024

upregulates receptor activator of NF-κB ligand (RANKL) secretion by local osteogenic cells, thus causing bone destruction (i.e., osteolysis) and favoring tumor cell survival and expansion in the bone marrow microenvironment. This suggests that BDNF may also play a role in the development of lytic lesions associated with other hematological and non-hematological tumors as well as in benign skeletal diseases characterized by abnormally high bone remodeling activity. A well-known example of the latter is fibrous dysplasia of bone (FD, OMIM 174800), a genetic skeletal dysplasia due to gain-of-function mutations of the alpha subunit of the stimulatory G protein (Gsα) [19], encoded by *GNAS* gene, that during skeletal growth cause the development of fibro-osseous lesions in one (monostotic FD) or multiple (polyostotic FD) skeletal segments [20,21]. Independent of their number and topographic distribution, FD lesions always feature uncontrolled osteoclast formation and bone resorption that affect both pre-existing, normal bone as well as newly formed, pathological bone, leading to osteolysis, bone fragility, deformities and recurrent fractures, often associated with chronic pain [20,22,23]. Based on studies performed on FD patients and different transgenic mouse models of the disease, enhanced osteoclastogenesis within FD lesions is commonly ascribed to local secretion of RANKL by the fibrous tissue [24,25].However, the potential role of factors other than RANKL, able to modulate, either directly or indirectly, osteoclast formation and/or activity has remained poorly investigated. We previously observed that *BDNF* transcripts are expressed in human FD, especially in lesions characterized by extensive bone resorption and increased vascularization [26]. This finding, which is consistent with the osteogenic nature of the FD tissue and with the regulation of BDNF secretion by the Gsα/cAMP pathway [27] strongly suggests that BDNF may be implicated in the development of the osteolytic lesions that characterize the disease. In this study, we attempted to address this question by investigating the pattern of expression of BDNF and its receptor TRKB in human FD bone biopsies and in skeletal segments of the EF1α-Gsα^{R201C} transgenic mouse model (FD mice) [25,28]. We also performed a pilot study in which we treated FD mice with an anti-BDNF antibody to assess the effect of BDNF inhibition on osteoclast formation and bone resorption within the pathological tissue. Overall, our data suggest that BDNF contributes to the pathology of FD and may be a novel therapeutic target for the disease.

2. Materials and methods

2.1. *EF1α-Gsα^{R201C} mice and anti-BDNF treatment*

The generation of the FD mouse model used in this study was previously reported [28]. All studies were performed in compliance with relevant Italian laws and Institutional guidelines and all procedures were IACUC approved.

Mouse genotyping was performed using the oligonucleotide sequences reported in Table S1. Wild type (WT) littermates were used as control. All mice were maintained at standard environmental conditions (temperature 22–25 °C, humidity 40–70 %, 12:12 dark/light photoperiod) with food and water provided ad libitum. The development of the skeletal phenotype in FD mice was assessed by radiographic analysis using Faxitron MX-20 Specimen Radiography System (Faxitron X-ray Corp., Wheeling, IL, USA) set at 24–25 kV for 6–8 s with Kodak MINR2000 films.

For BDNF inhibition experiments, 5-month-old FD male mice were treated with either an anti-BDNF monoclonal antibody (αBDNF, clone B30, Creative Biolabs, Shirley, NY, USA) at a dose of 1 mg/kg or with PBS as vehicle (Veh), via intraperitoneal injection, twice a week for 3 weeks. The selection of the B30 anti-BDNF monoclonal antibody and of the dose for in vivo experiments was based on the study of Stack and colleagues [29] reporting the development of this highly specific neutralizing antibody.

2.2. *Serum BDNF analysis*

Blood was collected from the mouse facial vein and allowed to clot for 30 min at room temperature. Samples were then centrifuged at 2000 ×*g* for 10 min at 4 °C and mature BDNF was measured using Mature BDNF Rapid™ ELISA Kit (Biosensis, Thebarton, Australia) according to manufacturer's instructions.

2.3. *Gene expression analysis*

Human bone biopsies were received as surgical waste from FD patients and healthy donor (HD). They were used in accordance with the Declaration of Helsinki and its later amendments, and the study was approved by the local Ethical Committee (Rif. 7311 – Prot.0706/2023).

Mouse tissues were collected after euthanasia by carbon dioxide inhalation. Quadriceps, whole brains, right femurs and tail vertebrae were immediately harvested and snap-frozen in liquid nitrogen.

Both human and mouse tissues were kept at −80 °C until use. Following homogenization by Mikro-Dismembrator U (Gottingen, Germany) total RNA was isolated using the TRI Reagent® (Thermo Fisher Scientific, Waltham, USA) protocol. cDNA was obtained by using PrimeScript RT Reagent Kit (Takara, Japan) and quantitative PCR (qPCR) analysis was performed on a 7500 Fast Real-Time PCR System (Applied Biosystem, Waltham, MA, USA) using PowerUP Sybr Green (Thermo Fisher Scientific) to amplify genes of interest with specific primers (Table S1). Gene expression levels were normalized to *Gapdh* or *Actb* expression.

2.4. *Clustering analysis*

Clustering analysis was performed using gene expression data available at NCBI GEO: GSE176243. Expression data were normalized as previously described in Persichetti et al. [26] and were log2 transformed for downstream analyses. Osteoclast-related gene enrichment was performed using three different datasets (BioGPS Mouse Cell Type and Tissue Gene Expression Profiles, PanglaoDB_markers_27_Mar_2020, GeneRIF Biological Term Annotations).

Hierarchical clustering analysis of samples and genes was performed using "heatmap.2" function in R by employing "gplots" package in R software.

2.5. *Western blot analysis*

Single tail vertebrae were homogenized with RIPA buffer (Sigma Aldrich, Saint Louis, MO, USA) and total proteins were collected after centrifugation at 20000 RCF (relative centrifugal force) for 15 min. Total protein amount was determined using the BCA protein assay (Thermo Fisher Scientific). Laemmli sample buffer (BioRad Laboratories, CA, USA) was added to lysates and samples were boiled for 5 min at 95 °C. Denatured samples were electrophoresed in 4–20 % tris glycine pre-cast polyacrylamide gels (Thermo Fisher Scientific) and transferred onto PVDF membranes (Amersham, NY, USA). Primary antibodies (anti-TRKB, #AF1494, R&D System, MN, USA; anti-BDNF, #GTX132621, GeneTex, CA, USA; anti-αTUBULIN #T8203 Sigma Aldrich) were incubated overnight at 4 °C and secondary antibodies were incubated for 1 h at room temperature. Signals were detected with horseradish peroxidase (HRP)-conjugated secondary antibodies and enhanced chemiluminescence (Thermo Fisher Scientific). Chemiluminescent images of immunodetected bands were recorded with the Syngene G-box system (Syngene Bioimaging, MD, USA), and immunoblot intensities were quantitatively analyzed using ImageJ Software (NIH, Bethesda, MD, USA). TRKB and BDNF expression levels were normalized to αTUBULIN expression.

2.6. Histology and histochemistry

Histological studies on human FD were performed on the same archival formalin-fixed, decalcified and paraffin embedded (FFDPE) bone biopsies used in our previous work [26].

Mouse skeletal segments were collected after euthanasia, fixed with 4 % formaldehyde in PBS pH 7.4 for 48 h, decalcified with 0.5 M EDTA at 4 °C for 3–7 days and embedded in paraffin as per standard procedure. Three-μm-thick sections were cut from paraffin blocks and used for histology, histochemistry, immunohistochemistry and histomorphometry.

Histochemistry for Tartrate-Resistant Acid Phosphatase (TRAP) was performed using Sigma Aldrich reagents (Sigma Aldrich) as previously reported [30]. Briefly, Naphtol AS-BI phosphate was dissolved in *N*,*N*-dimethylformamide and mixed with a solution of acetate buffer, tartaric acid and Fast Garnet. After deparaffinization, sections were rehydrated and then incubated in the TRAP solution at 37 °C for 45 min.

2.7. Immunohistochemistry

Immunohistochemistry for BDNF on human FD was performed on samples from patients 2 and 7 used in our previous work [26]. Both human and mouse bone samples were incubated with an anti-BDNF antibody (#GTX132621, GeneTex) applied at a dilution of 1:200 in PBS overnight at 4 °C. After incubation with the primary antibody and repeated washing with PBS, sections were exposed for 30 min to biotin-conjugated polyclonal swine anti-rabbit IgG (#E0353, Agilent Dako, Santa Clara, CA, USA) 1:500 in PBS and then for 30 min to peroxidase-conjugated streptavidin (#P0397, Agilent Dako) 1:1000 in PBS. The peroxidase reaction was developed using DAB substrate kit (SK-4105, Vector Laboratories, Burlingame, CA, USA).

2.8. Histomorphometry

Histomorphometry on mouse samples was conducted on paraffin sections from femurs, lumbar and tail vertebrae as described previously [25,31]. Analyses were performed in a blinded fashion by a single experimentalist, using ImageJ software [32] and following standard procedure and nomenclature [33,34]. Briefly, the region of interest was drawn 300 μm below the growth plate of all the bone segments analyzed. Sirius red-stained sections were used to measure the volume of trabecular bone per tissue volume (BV/TV) and fibrous tissue per tissue volume (Fb.V/TV); hematoxylin/eosin (H&E)-stained sections were used to evaluate the volume of bone marrow adiposity per tissue volume (Ad.V/TV), osteoblast number per bone surface (N.Ob/BS) or tissue area (N.Ob/TA), and osteoblast surface per bone surface (Ob.S/BS); TRAP-stained sections were analyzed to measure osteoclast number per bone surface (N.Oc/BS) or tissue area (N.Oc/TA), and osteoclast surface per bone surface (Oc.S/BS) in femurs. In caudal vertebrae, the parameters of osteoclast area per tissue area (Oc.Ar/TA) and the mean osteoclast size (Oc. Size) were also measured.

Histomorphometry on human biopsies was conducted by counting mono and multinucleated TRAP-positive osteoclasts in at least 10 fields of the histological section, and by evaluating N.Oc/TA, Oc.Ar/TA and Oc. Size.

2.9. BMSCs isolation and osteogenic differentiation

Bone marrow stromal cells (BMSCs) were isolated from 3-month-old EF1α-Gsα^{R201C} mice. Briefly, hind limb long bones were dissected after euthanasia and kept in warm αMEM (Sigma-Aldrich) supplemented with 1 % penicillin/streptomycin (P/S, Sigma-Aldrich). After removal of soft tissues, the extremities of femurs and tibiae were cut to expose the bone marrow. Using a syringe filled with sterile αMEM, bone marrow was flushed out and cells were resuspended in αMEM supplemented with 20 % FBS (Thermo Fisher Scientific), 1 % L-glutamine (L-gln, Sigma-Aldrich) and 1 % P/S (Sigma-Aldrich) and plated in a 150 mm culture dish to allow adhesion of BMSCs to the plastic. After expansion, BMSCs were plated in 24-well plates at the density of $2{,}5 \times 10^4$ cells/well and incubated for 14 days in an osteogenic medium containing DMEM supplemented with 10 % FBS, 1 % L-gln, 1 % P/S (Thermo Fisher Scientific), 4 mM β-glycerophosphate and 50 μg/ml of Ascorbic Acid (Sigma-Aldrich). For gene expression analyses during BDNF inhibition, BMSCs were treated at day 14 with αBDNF at the concentration of 0 (Veh), 0,1 μg/ml and 1 μg/ml for 6 h in osteogenic medium without FBS. After antibody incubation, cells were lysed with Trizol and collected for RNA isolation.

2.10. Statistical analysis

Data are shown as bar graph with overlapping dots, and mean ± SEM are reported. Each dot represents an individual value. To compare two groups a student *t*-test was used, while a One-way ANOVA with multiple comparison test was used to compare three groups. Two-way ANOVA with Tukey's multiple comparison test was used to detect statistical differences between WT and EF1α-Gsα^{R201C} mice at different ages. Correlation was analyzed using the Pearson correlation test. In all statistical analyses a p-value <0.05 was considered statistically significant. Graphs and statistical tests were performed using GraphPad Prism version 9 (GraphPad Software, La Jolla, CA, USA).

3. Results

3.1. BDNF is produced by osteogenic cells in human FD lesions

In a previous study, we performed a wide gene expression analysis on FFDPE human FD bone biopsies and identified two clusters with distinct patterns of gene expression [26]. *BDNF* was noticed as one of the most differentially expressed genes. Further analysis showed that *BDNF* transcripts and those of *TRKB* (a BDNF receptor encoded by the *NTRK2* gene) were enriched preferentially in one cluster of samples (Fig. 1A, Cluster 1). In this group, genes involved in the mineral matrix homeostasis, such as matrix metalloproteinases (MMPs) and *FGF23,* and some of the most common genes related to osteoclast formation and function such as *CSF1R* were also enriched (Fig. 1A Cluster 1 and Fig. S1A). From an histological perspective, these samples presented a brisk bone remodeling activity and a high number of osteoclasts (Fig. 1B,C Cluster 1). Accordingly, we observed a positive correlation between the number of osteoclasts and *BDNF* expression, while no correlation was observed with *NTRK2* (Fig. S1B). Immunohistochemistry performed on biopsies with higher expression of *BDNF* transcripts, revealed that BDNF was widely distributed throughout lesions, being produced either by undifferentiated stromal cells within the fibrotic marrow and by more differentiated, bone-forming cells on the surface of bone trabeculae (Fig. 1D, Cluster 1). In contrast, BDNF was found to be expressed only by few osteoblasts in samples that showed a lower level of its transcript (Fig. 1D, Cluster 2).

We further supported these data by analyzing the expression of *BDNF* and its receptor *TRKB* in frozen human FD bone tissue. We observed that the levels of both transcripts were higher in FD compared to HD, although high variability was observed among FD samples (Fig. 1E). Altogether these data indicate that FD bone lesions produce BDNF and suggest a potential role for BDNF/TRKB axis in their molecular pathogenesis.

3.2. BDNF is expressed in mouse FD lesions

We then analyzed the expression of BDNF and TRKB in bone segments of FD mice. Since they did not show sex-specific difference in *Bdnf* and *Ntrk2* gene expression in the skeleton (Fig. S2A), only male mice were used in all the experiments.

Gene expression analysis performed on tail vertebrae of WT and FD

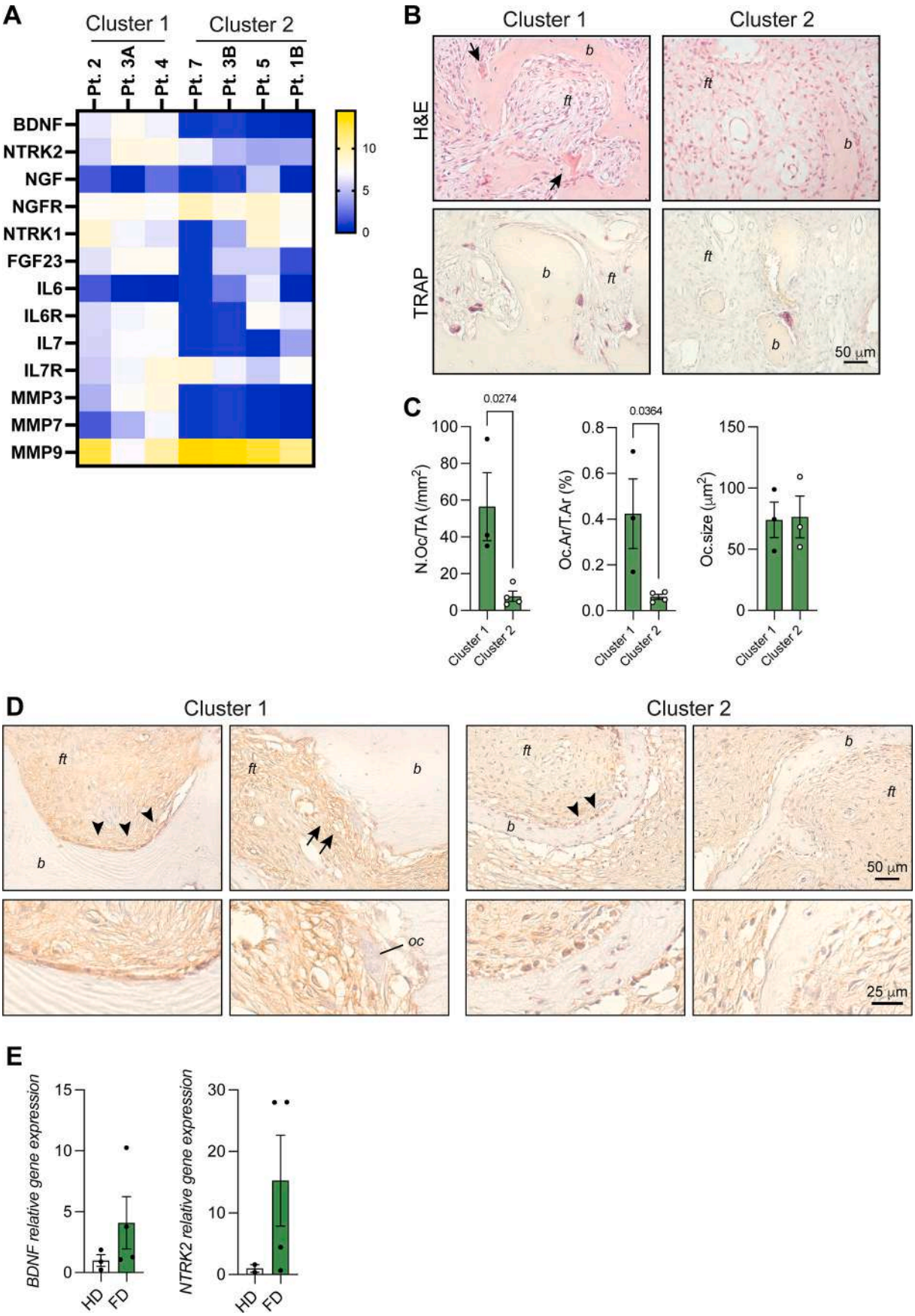

(caption on next page)

Fig. 1. BDNF expression in human FD lesions. **A)** Representative panel of genes from Nanostring nCounter multiplex gene expression analysis performed on FFDPE human FD bone biopsies. The two clusters of biopsies are shown according to Persichetti et al. [26] **B)** Representative H&*E*- and TRAP-stained tissue sections of human FD samples in Cluster 1 and Cluster 2, showing enrichment of osteoclast cells (arrows and red stains) in Cluster 1. **C)** Comparative histomorphometry of osteoclast parameters between Cluster 1 and Cluster 2. N.Oc/TA: number of osteoclasts per tissue area. Oc.Ar/TA: osteoclast area per tissue area. Oc.Size: mean osteoclast size **D)** Immunolocalization of BDNF in representative FD lesions of Cluster 1 and Cluster 2, demonstrating BDNF expression in osteoblasts (arrowheads) and fibrous tissue (arrows). b = bone; ft = fibrous tissue; oc = osteoclast. **E)** qPCR gene expression analysis of *BDNF* and *NTRK2* performed on fresh HD and FD bone tissues. *GAPDH* was used as housekeeping gene for normalization. Data are presented as dot plots with column bars showing all the experimental samples. Statistical analysis was performed using Student *t*-test. (For interpretation of the references to colour in this figure legend, the reader is referred to the web version of this article.)

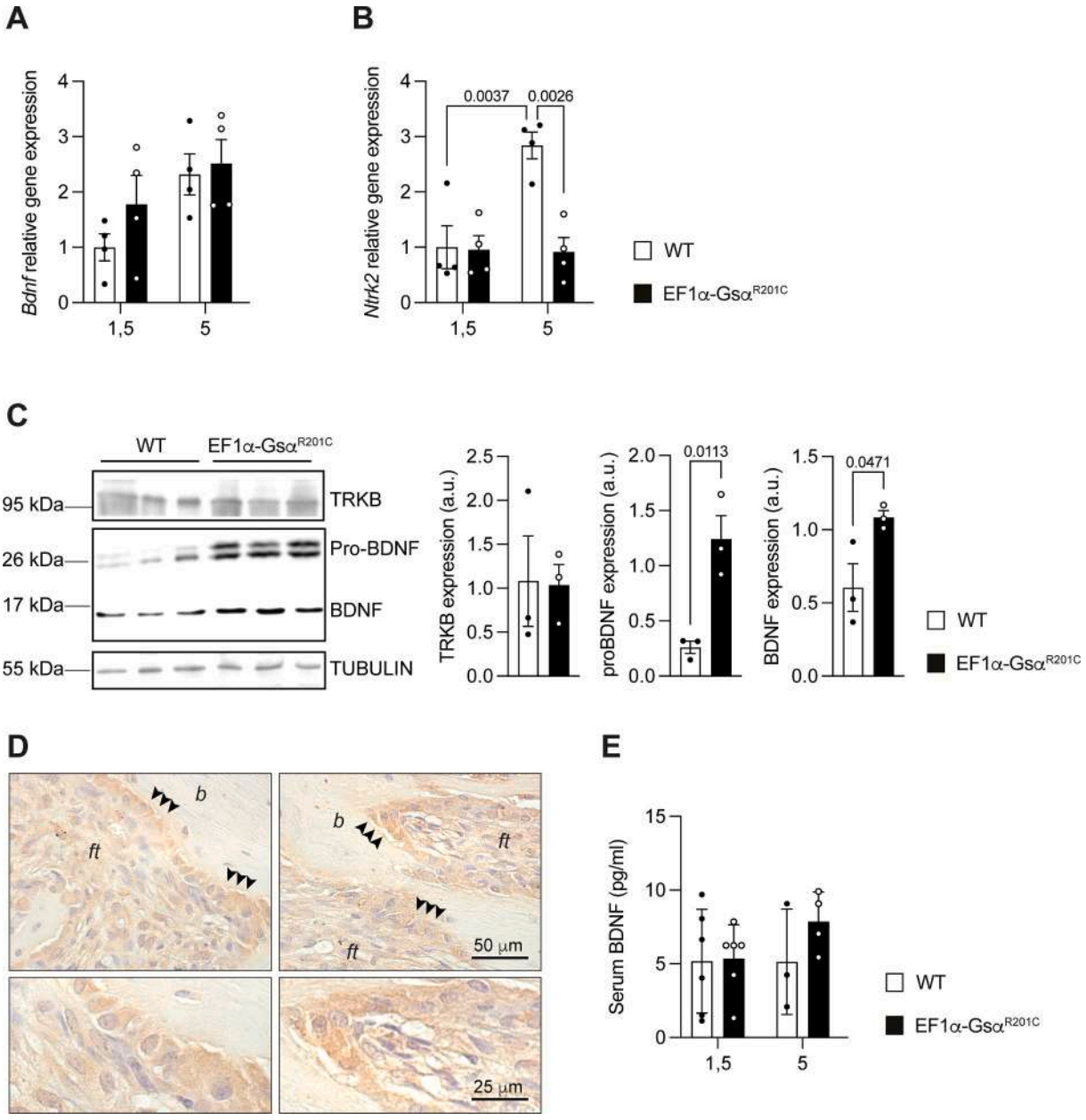

Fig. 2. BDNF expression in EF1α-Gsα^{R201C} mice. **A, B)** *Bdnf* (**A**) and *Ntrk2* (**B**) relative gene expression in tail vertebrae of 1,5- and 5-month-old WT and EF1α-Gsα^{R201C} male mice. *Actb* was used as housekeeping gene for normalization. **C)** Western blot analysis showing BDNF, both the precursor form (pro-BDNF) and the mature form (BDNF), and TRKB expression in the tail vertebrae of 5-month-old WT and EF1α-Gsα^{R201C} male mice. Densitometric analysis of immunoblots is reported. TRKB, proBDNF and BDNF expression levels were normalized on α-Tubulin levels and reported in the graph as arbitrary units (a.u.). **D)** Immunolocalization of BDNF in FD lesions from 5-month-old EF1α-Gsα^{R201C} male mice, showing strong labeling in the osteoblast population (arrowheads). b = bone; ft = fibrous tissue. **E)** Circulating BDNF levels in WT and EF1α-Gsα^{R201C} male mice at 1,5 and 5 months of age. Data are presented as dot plots with column bars showing all the experimental samples. Statistical analysis was performed using Two-Way ANOVA or Student *t*-test depending on the number of groups to compare. *P* values lower than 0.05 are shown above each graph.

mice at 1,5 and 5 months of age, showed an age-dependent increase in the levels of *Bdnf* in all mice (Fig. 2A). No differences were observed between WT and FD mice at these two ages (Fig. 2A). On the other hand, while the expression of *Ntrk2* (TRKB gene) increased significantly over time in control mice, this was not observed in FD mice (Fig. 2B). Indeed, *Ntrk2* levels were similar in 1,5-month-old FD and WT mice, while resulted markedly decreased in FD mice compared to controls at 5 months of age (Fig. 2B).

We then performed a WB analysis on tail vertebrae of 5-month-old mice. It is known that BDNF protein is first synthesized as a precursor form (pre-pro-BDNF), and then undergoes cleavages toward pro-BDNF and mature BDNF [35]. In our samples, WB analysis revealed an increase in pro- and mature BDNF in FD mice compared to control littermates (Fig. 2C). No differences were observed in TRKB levels between WT and FD mice (Fig. 2C). The analysis of the spatial pattern of BDNF immunolabeling within mouse FD lesions showed wide overlap with that observed in human samples, being diffused throughout the pathological fibro-osseous tissue (Fig. 2D), especially in osteoblasts. To assess whether differences could be also detected in circulating BDNF, we collected blood from FD and control littermate mice. The levels of BDNF were overall similar in serum of FD and control mice. Slightly higher concentrations were observed in 5-month-old FD mice compared to controls, but this result did not reach statistical significance (Fig. 2E).

3.3. BDNF inhibition reduces the fibro-osseous tissue in mouse FD lesions

To assess the contribution of BDNF activity to the tissue pathology of FD, 5-month-old FD male mice with radiographically detectable lesions were treated for 21 days with a blocking anti-BDNF antibody (αBDNF, Fig. 3A). The specificity of the antibody was assayed by measuring circulating BDNF levels. No BDNF could be detected in the serum at the end of the experiment, thus confirming the binding of the recombinant antibody (Fig. S2B). At the end of the treatment, radiographic analysis failed to reveal major changes in bone density of BDNF-inhibited mice at either affected (Fig. 3B) or unaffected (data not shown) skeletal sites.

However, histological and histomorphometric analyses revealed changes in the microscopic features of the FD tissue, with a preferential effect at specific skeletal sites. Indeed, in lesions of the femur, which, of note, is one of the first and most frequently affected skeletal sites in FD patients and mice, the amount of fibrous tissue and the trabecular bone mass were reduced in mice that received αBDNF compared to Veh-treated animals (Figs. 3C, F and S2C). In addition, some hematopoietic cells could also be detected in the inter-trabecular spaces (Fig. 3C). In contrast, no differences in the percentage of fibrous tissue volume and trabecular bone mass were observed with αBDNF treatment in the other two bone segments analyzed, lumbar and tail vertebrae (Fig. 3D-F and S2C). No difference was observed in bone marrow adiposity of αBDNF-treated mice (Fig. S2D). Overall, these results indicate that inhibition of BDNF was able to halt or reduce bone resorption and fibro-osseous tissue formation in FD although the effect was not homogeneous across the skeleton.

3.4. Inhibition of BDNF activity reduces osteoclast number in mouse FD lesions

The αBDNF antibody exerted an inhibitory effect on bone resorption. TRAP histochemistry performed on femurs and tail vertebrae showed a lower representation of mono and multinucleated osteoclasts, both on bone surfaces and within the fibrous tissue in bone segments from αBDNF-treated mice compared to animals from the Veh group (Fig. 4A, B). Histomorphometry confirmed that osteoclast number as well as total osteoclast area, were significantly reduced in mice receiving the treatment (Fig. 4C, D), while no differences in the osteoclast size were found (Fig. 4D).

To better evaluate the effect of the αBDNF antibody on the osteoclastogenic activity within the FD tissue, we analyzed the expression of osteoclastogenic genes in whole vertebrae. We observed a significant reduction in the level of *Rankl* transcript upon BDNF inhibition and a reduced expression, albeit not significant, of other osteoclast-related genes such as *Rank, Mmp9 and Ctsk* (Fig. 4E).

3.5. BDNF inhibition reduces osteogenesis in FD mice

In order to further dissect the cellular response to BDNF inhibition in FD, we evaluated the osteogenic compartment in femoral lesions of αBDNF treated mice. Osteoblast number and surface were significantly reduced in treated mice compared to the Veh group (Fig. 5A, B).

Gene expression analysis of selected osteogenic markers revealed reduced levels of *Runx2* and *Alpl* although these results did not reach statistical significance, likely due to the high variability observed in this experiment (Fig. 5C). We further investigated the effect of αBDNF treatment on the osteogenic differentiation of mouse marrow osteoprogenitor cells (bone marrow stromal cells, BMSCs). We observed that BDNF inhibition altered the osteogenic program of mouse BMSCs, as the expression of *Runx2*, *Sp7*, *Alpl* and *Bglap* was significantly reduced in αBDNF-treated cells induced to osteoblastic differentiation compared to untreated osteogenic cultures (Fig. 5D). These results are consistent with the reported positive regulatory function of BDNF on osteogenesis [12–14] and suggest that this neurotrophin could be important in regulating bone formation within the FD fibro-osseous tissue.

3.6. BDNF inhibition does not impair brain and muscle Bdnf expression

No adverse events were detected during the treatment of FD mice with αBDNF. Inhibition of BDNF activity did not interfere with the mouse weight and growth (Fig. S3A) and necropsy confirmed that size and morphology of their organs were comparable to those of Veh-treated mice (data not shown). To better assess the extra-skeletal effects of BDNF inhibition, we performed molecular analysis on two major body sources of the neurotrophin, brain and skeletal muscle. In brain samples, expression of *Bdnf* in FD mice was similar to that of WT littermates and was not affected by BDNF inhibition (Fig. 6A). In skeletal muscle, the levels of *Bdnf* were significantly lower in FD mice compared to WT mice (Fig. 6B). Surprisingly, BDNF inhibition seemed to restore the level of muscle *Bdnf* (Fig. 6B) without affecting the expression of other genes involved in skeletal muscle function such as *Il6* and *Pgc1a* (Fig. S3B).

4. Discussion

Increasing evidence suggests that neurotrophins are involved in bone development, homeostasis and disease [11,36,37]. In this study, we show that BDNF contributes to the abnormal osteoclastogenesis that underlies the tissue pathology and the clinical morbidity of FD. Our work provides a new example of the role of neurotrophins in skeletal physiopathology as well as a new insight, with potential therapeutic implication, into the pathogenetic mechanisms of FD.

BDNF is thought to participate in the regulation of different cellular processes during skeletal development and growth. Previous work showed that both BDNF and its receptor are highly expressed in the femoral growth plate, especially in the proliferating and mature zone, and in active osteoblasts at sites of endochondral and membranous bone formation [11]. This pattern of expression, further supported by in vitro work, suggested that BDNF is an important regulator of chondrocyte and osteoblast differentiation, likely through an autocrine mechanism.

In skeletal diseases, the best-defined role of BDNF relates to its primary activity as a local promoter and central sensitizer of pain, especially in pain conditions caused by bone cancer and trauma [38–42]. In contrast, the potential participation of BDNF in skeletal pathology through a direct or indirect effect on bone cell differentiation and/or function is, as yet, poorly understood. Most work in this field explored the connection between BDNF and osteogenesis, especially in conditions of reduced bone mass [43] and during fracture healing [12–14,44–46].

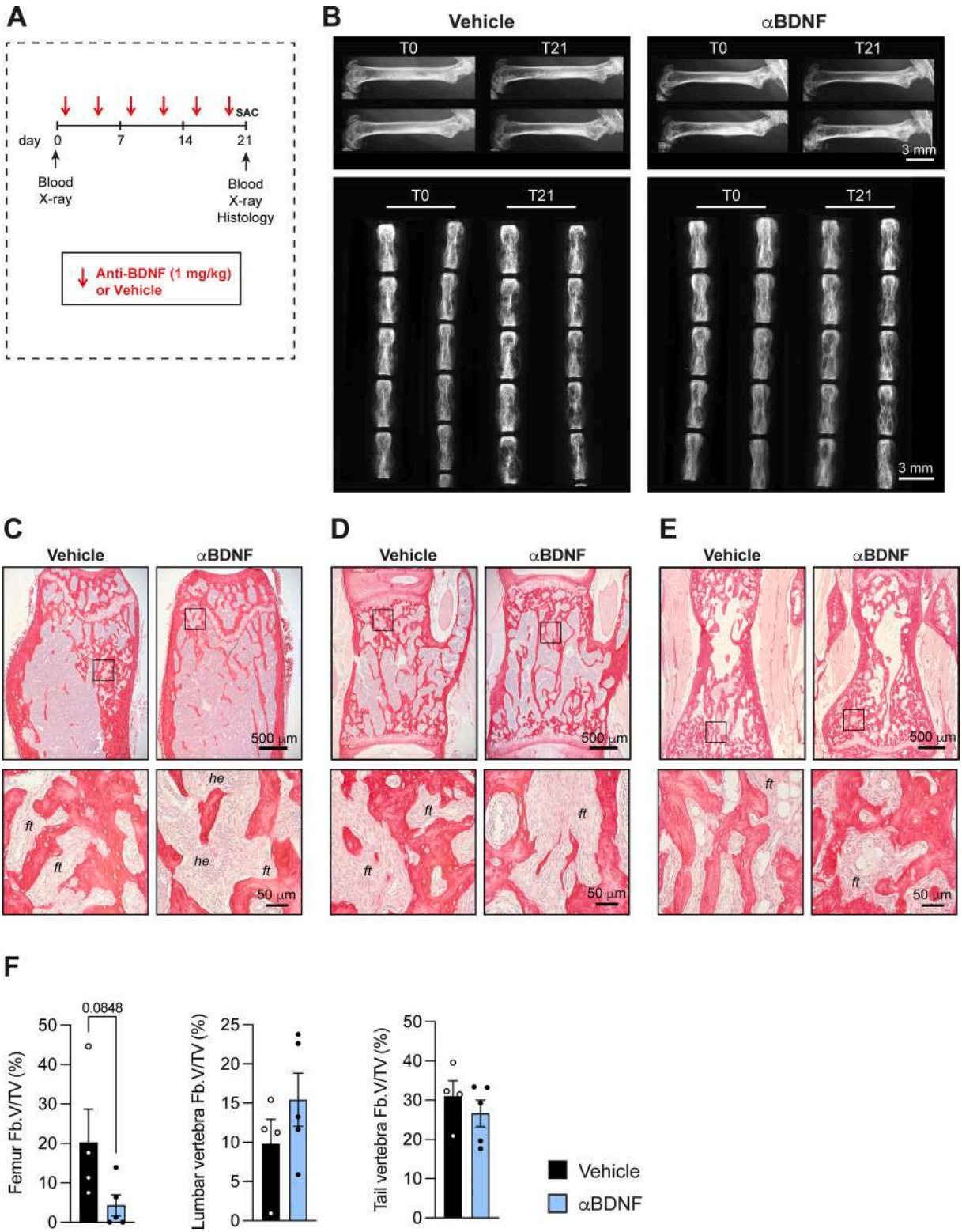

Fig. 3. BDNF inhibition in EF1α-Gsα^{R201C} male mice. **A)** Experimental scheme of anti-BDNF treatment in 5-month-old EF1α-Gsα^{R201C} mice. **B)** Radiographic analysis of femurs and tail vertebrae of EF1α-Gsα^{R201C} mice treated with Veh or αBDNF at the beginning (T0) and at the end (T21) of treatment. **C-E)** Sirius red-stained tissue sections of femurs (**C**), lumbar (**D**) and tail (**E**) vertebrae of Veh- and αBDNF-treated EF1α-Gsα^{R201C} mice. ft = fibrous tissue; he = hematopoietic marrow. **F)** Histomorphometric analysis of fibrous tissue in femurs, lumbar and tail vertebrae of Veh- and αBDNF-treated EF1α-Gsα^{R201C} mice. Fb.V/TV: fibrous tissue volume per tissue volume. Data are presented as dot plots with column bars showing all the experimental samples. Statistical analysis was performed using Student *t*-test. (For interpretation of the references to colour in this figure legend, the reader is referred to the web version of this article.)

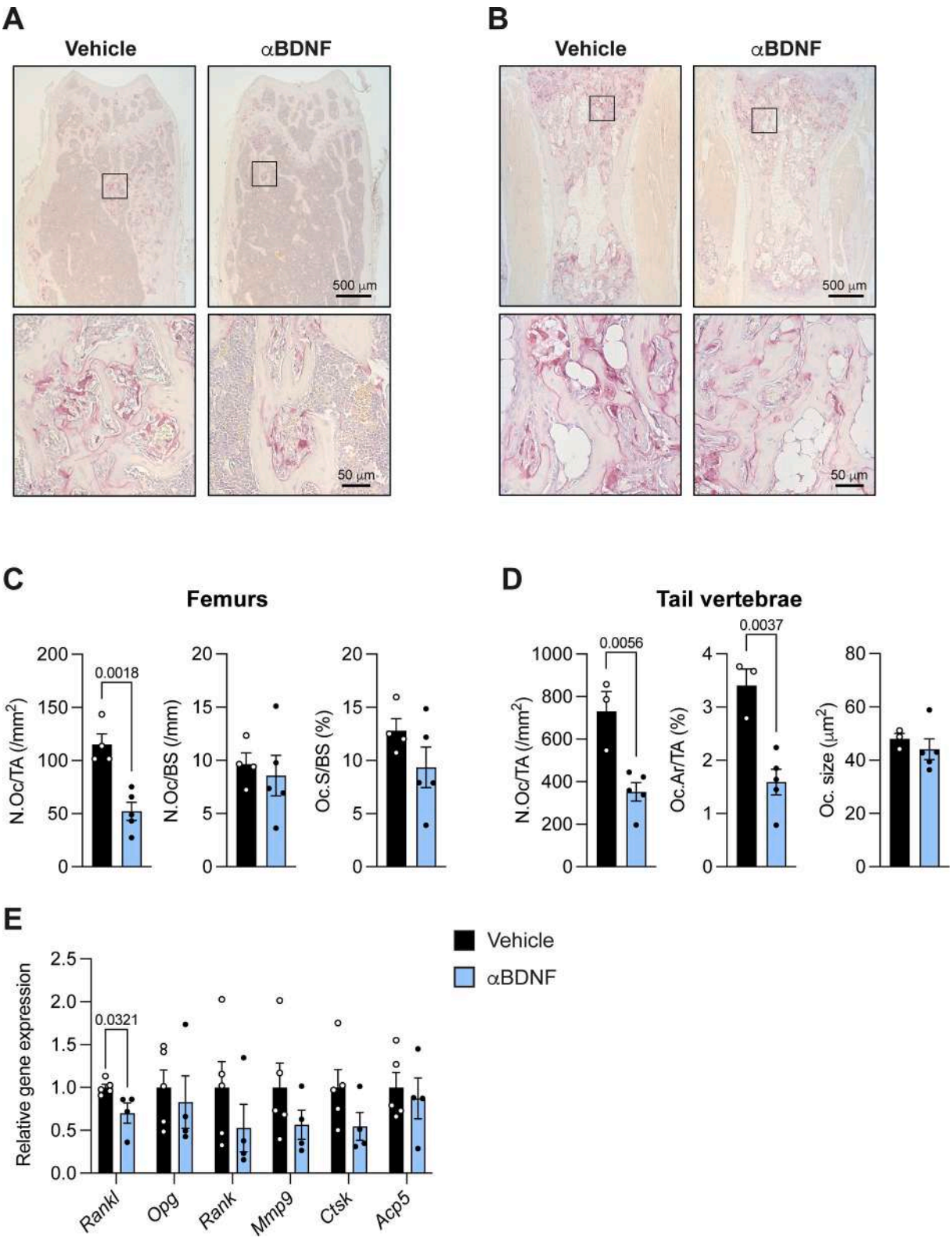

Fig. 4. Osteoclasts in αBDNF-treated EF1α-Gsα^{R201C} male mice. **A, B)** TRAP histochemistry performed on tissue sections of femurs (**A**) and tail vertebrae (**B**) of Veh- and αBDNF-treated EF1α-Gsα^{R201C} mice. **C, D)** Histomorphometric analysis of osteoclast parameters in femurs (**C**) and tail vertebrae (**D**) of EF1α-Gsα^{R201C} mice treated with Veh or αBDNF. N.Oc/TA: number of osteoclasts per tissue area. N.Oc/BS: number of osteoclasts per bone surface. Oc.S/BS: osteoclast surface per bone surface. Oc.Ar/TA: osteoclast area per tissue area. Oc. size: mean osteoclast size. **E)** Expression of osteoclast-related genes in tail vertebrae of Veh and αBDNF-treated EF1α-Gsα^{R201C} mice. *Gapdh* was used as housekeeping gene for normalization. Data are presented as dot plots with column bars showing all the experimental samples. Statistical analysis was performed using Student *t*-test and *p* values lower than 0.05 are shown above each graph.

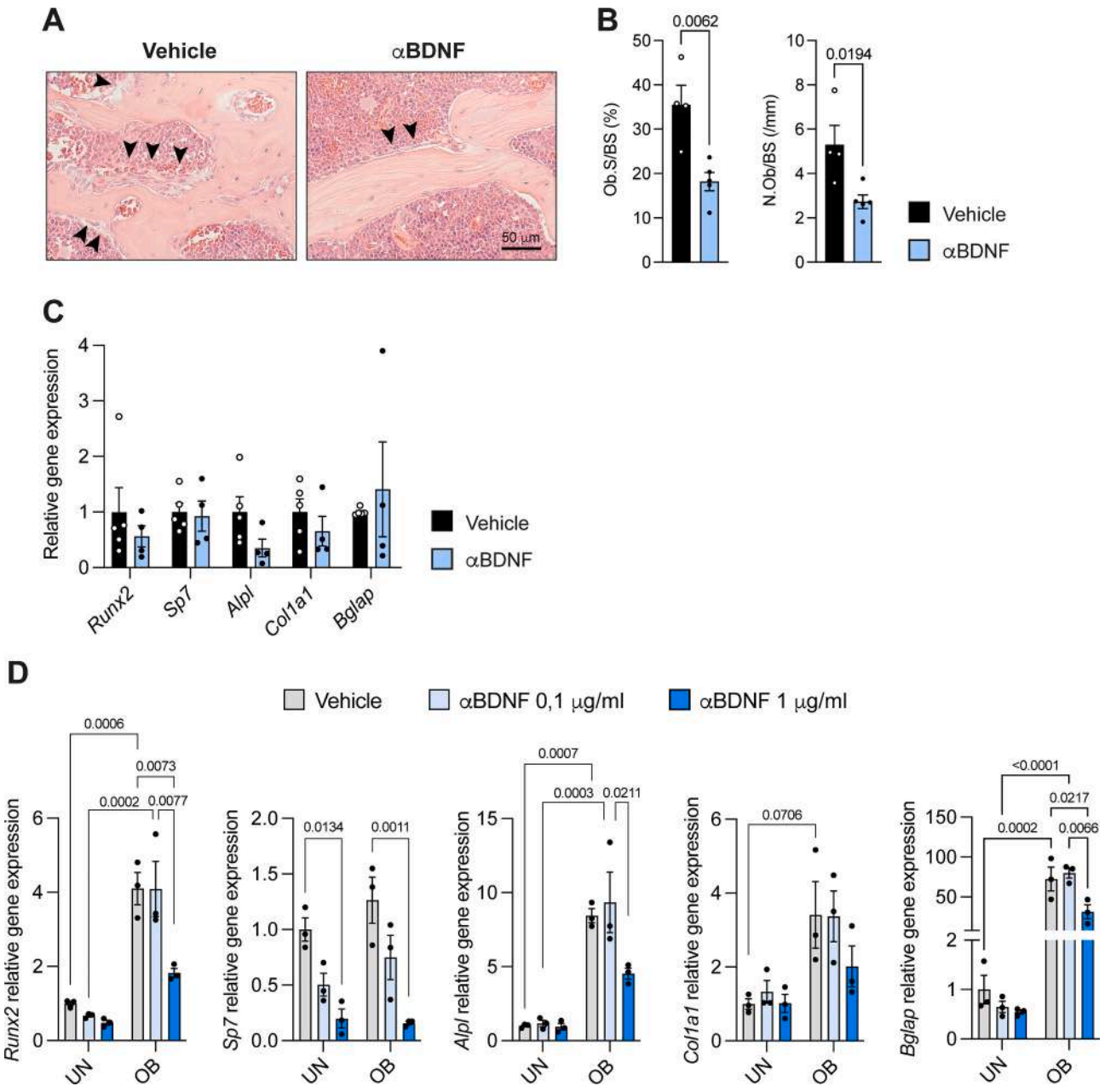

Fig. 5. Osteogenesis in αBDNF-treated EF1α-Gsα^{R201C} male mice. **A, B)** H&E-stained tissue sections (**A**) and histomorphometric analysis of osteoblast parameters (**B**) in femurs of Veh- and αBDNF-treated EF1α-Gsα^{R201C} mice. Arrowheads: osteoblasts, Ob.S/BS: osteoblast surface per bone surface. N.Ob/BS: number of osteoblasts per bone surface. **C)** Gene expression of osteoblast-related genes in Veh and αBDNF-treated EF1α-Gsα^{R201C} mice. **D)** Relative gene expression of osteogenic genes in undifferentiated (UN) and osteogenic-induced (OB) BMSCs treated with Veh or two different concentrations of αBDNF. Data are presented as dot plots with column bars showing all the experimental samples. In gene expression experiments, *Gapdh* was used as housekeeping gene for normalization. Statistical analysis was performed using Two-Way ANOVA or Student *t*-test depending on the number of groups to compare. *P* values lower than 0.05 are shown above each graph.

In contrast, the studies that investigated the role of the neurotrophin in skeletal disorders with abnormal bone resorption, are few and focused essentially on neoplastic conditions [15–18] in which BDNF is secreted by tumor cells into the bone marrow microenvironment. Thus, our study provides the first evidence of the involvement of BDNF produced by bone cells in the pathogenesis of a primary and benign osteolytic bone disease.

We demonstrated that BDNF and TRKB were both produced in the pathological tissue of human and mouse FD and that in mice, the levels of the protein were higher in affected skeletal segments compared to wild type bone.

Most important, we demonstrated that BDNF inhibition reduced the number of osteoclasts in mouse FD lesions. Previous studies reported that the pro-osteoclastogenic activity of BDNF is dependent on the stimulation of RANKL secretion by osteogenic cells through the use of different molecular mediators and pathways [15–18]. Accordingly, we observed a reduction in the levels of *Rankl* mRNA in mouse skeletal segments with FD lesions upon treatment with the anti-BDNF antibody. In contrast with the effect on osteoclast number, we did not observe significant changes in the size of individual osteoclasts, suggesting that the αBDNF treatment did not modulate the fusion ability of their progenitor cells. Furthermore, in a previous study on osteolytic lesions associated with Multiple Myeloma, Sun and colleagues showed that BDNF did not alter the activity of mature osteoclasts [15]. Thus, based on previous data and our results, it may be assumed that BDNF enhances bone resorption by affecting specifically the number of multinucleated

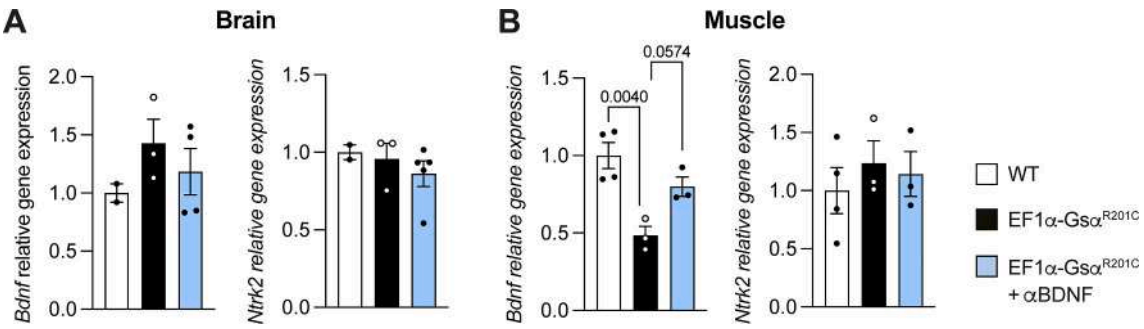

Fig. 6. A, B) *Bdnf* and *Ntrk2* relative gene expression in brain (**A**) and muscle (**B**) of WT and EF1α-Gsα^{R201C} male mice treated with Veh or αBDNF. *Actb* was used as housekeeping gene for normalization. Data are presented as dot plots with column bars showing all the experimental samples. Statistical analysis was performed using One-Way ANOVA with multiple comparison test and *p* values close to and lower than 0.05 are shown above each graph.

osteoclasts.

Consistent with its expression during osteogenesis, the inhibition of BDNF in FD mice also associated with a reduction in the number and surface of osteoblasts, a change that likely provided a further indirect mechanism for the reduction of RANKL levels in the local microenvironment. Altogether, the combined effects of BDNF inhibition on the osteoclastogenic and osteogenic activity led to significant reduction in the fibro-osseous tissue of FD lesions. Although the histological changes were not homogeneous in all affected skeletal segments, it is important to note that they were clearly evident in FD lesions of segments such as the femur, which is one of the first and most frequently affected skeletal sites in FD, both in patients and mice.

In the absence of specific therapies able to inhibit the transcription of the mutated Gsα allele or to counteract the downstream molecular aberrations caused by its expression, anti-resorptive drugs represent the only rationale approach to contain the clinical morbidity and the progression of FD. Bisphosphonates (BPs) were widely used in FD patients, either as sporadic applications and in clinical trials, to inhibit bone resorption and possibly bone pain. Overall, no significant effect was observed on the growth of FD lesions whereas results on pain modulation were contrasting [47,48]. Likewise, no changes in the development and progression of the disease were detected in our FD mice treated with Zoledronic Acid [49]. Tocilizumab, a monoclonal antibody against the IL-6 receptor was tested in a clinical trial on FD patients not responding to BPs but neither changes in markers of bone turn-over nor reduction in bone pain were detected [50]. Currently, denosumab, a humanized antibody against the osteoclastogenic factor RANKL is the most promising medical approach for the treatment of the disease. In FD patients it was reported to improve bone turn-over markers and bone pain and to reduce the growth rate of bone lesions [51–53]. In FD mice a murine equivalent of denosumab (anti-mouse RANKL antibody) converted FD lesions into hyper-mineralized bone [25]. However, in both cases significant drawbacks of the treatment emerged, including a dramatic relapse of the disease with potentially life-threatening hypercalcemia at treatment withdrawal [25,54]. Therefore, a deeper understanding of the molecular mechanisms supporting osteoclast formation within FD lesions, including the BDNF-TRKB axis investigated in this study, seems to be very important to refine the current therapeutic approaches or to develop novel therapeutic strategies, based, for example, on the combined inhibition osteoclast formation and functions.

Finally, it is important to note that we also observed a reduced expression of BDNF in skeletal muscle of FD mice at baseline condition. To date, the only reported effect of the Gsα mutation in skeletal muscle refers to the development of benign myxoid tumors [55]. Given the relevance of BDNF in myogenesis, muscle metabolism and neuromuscular junction physiology [56] this finding suggests that skeletal muscle abnormalities may contribute to musculoskeletal impairment in FD patients thus calling for further investigation.

In conclusion, our data show that BDNF participates in the molecular pathogenesis of FD through indirect and direct mechanisms and encourages further long-term inhibition studies to better evaluate the potential value of BDNF as a novel therapeutic target for the disease.

CRediT authorship contribution statement

Biagio Palmisano: Writing – review & editing, Writing – original draft, Visualization, Validation, Methodology, Investigation, Funding acquisition, Formal analysis, Data curation, Conceptualization. **Giorgia Farinacci:** Methodology, Investigation, Data curation. **Federica Campolo:** Methodology, Data curation. **Chiara Tavanti:** Methodology, Data curation. **Alessia Stefano:** Methodology, Data curation. **Samantha Donsante:** Methodology. **Ernesto Ippolito:** Methodology. **Giuseppe Giannicola:** Methodology. **Mary Anna Venneri:** Writing – review & editing, Methodology. **Alessandro Corsi:** Writing – review & editing, Methodology. **Mara Riminucci:** Writing – review & editing, Writing – original draft, Supervision, Project administration, Funding acquisition, Conceptualization.

Fundings

This work was supported by Orphan Disease Center University of Pennsylvania in partnership with Fibrous Dysplasia Foundation (MDBR-21-110-FD, MDBR-23-010-FDMAS) to MR; Sapienza University (RM11916B839074A8, RM120172B8BF5C15) to MR; ECTS Basic/Translational Research Fellowship 2021 to BP.

Declaration of competing interest

The authors declare that they have no conflicts of interest to declare.

Data availability

Data will be made available on request.

Appendix A. Supplementary data

Supplementary data to this article can be found online at https://doi.org/10.1016/j.bone.2024.117047.

References

[1] S. Pezet, S.B. McMahon, Neurotrophins: mediators and modulators of pain, Annu. Rev. Neurosci. 29 (2006) 507–538.
[2] A. Acheson, et al., A BDNF autocrine loop in adult sensory neurons prevents cell death, Nature 374 (1995) 450–453.
[3] M. Bothwell, Functional interactions of neurotrophins and neurotrophin receptors, Annu. Rev. Neurosci. 18 (1995) 223–253.
[4] J.M. Grasman, D.L. Kaplan, Human endothelial cells secrete neurotropic factors to direct axonal growth of peripheral nerves, Sci. Rep. 7 (2017) 4092.

[5] M. Lommatzsch, et al., Abundant production of brain-derived neurotrophic factor by adult visceral epithelia. Implications for paracrine and target-derived neurotrophic functions, Am. J. Pathol. 155 (1999) 1183–1193.
[6] E. Labouyrie, et al., Expression of neurotrophins and their receptors in human bone marrow, Am. J. Pathol. 154 (1999) 405–415.
[7] O. Griesbeck, A.S. Parsadanian, M. Sendtner, H. Thoenen, Expression of neurotrophins in skeletal muscle: quantitative comparison and significance for motoneuron survival and maintenance of function, J. Neurosci. Res. 42 (1995) 21–33.
[8] M. Yamamoto, G. Sobue, K. Yamamoto, T. Mitsuma, Expression of mRNAs for neurotrophic factors (NGF, BDNF, NT-3, and GDNF) and their receptors (p75 ngfr, TrkA, TrkB, and TrkC) in the adult human peripheral nervous system and nonneural tissues, Neurochem. Res. 21 (1996) 929–938.
[9] D. Cassiman, Human and rat hepatic stellate cells express neurotrophins and neurotrophin receptors, Hepatology 33 (2001) 148–158.
[10] A. Wilkins, et al., Human bone marrow-derived mesenchymal stem cells secrete brain-derived neurotrophic factor which promotes neuronal survival in vitro, Stem Cell Res. 3 (2009) 63–70.
[11] T. Yamashiro, T. Fukunaga, K. Yamashita, N. Kobashi, T. Takano-Yamamoto, Gene and protein expression of brain-derived neurotrophic factor and TrkB in bone and cartilage, Bone 28 (2001) 404–409.
[12] K. Asaumi, T. Nakanishi, H. Asahara, H. Inoue, M. Takigawa, Expression of neurotrophins and their receptors (TRK) during fracture healing, Bone 26 (2000) 625–633.
[13] O. Kilian, et al., BDNF and its TrkB receptor in human fracture healing, Ann. Anat. 196 (2014) 286–295.
[14] Q. Liu, L. Lei, T. Yu, T. Jiang, Y. Kang, Effect of brain-derived neurotrophic factor on the neurogenesis and osteogenesis in bone engineering, Tissue Eng. Part A 24 (2018) 1283–1292.
[15] C.-Y. Sun, et al., Brain-derived neurotrophic factor is a potential osteoclast stimulating factor in multiple myeloma, Int. J. Cancer 130 (2012) 827–836.
[16] L.-S. Ai, et al., Inhibition of BDNF in multiple myeloma blocks osteoclastogenesis via down-regulated stroma-derived RANKL expression both in vitro and in vivo, PloS One 7 (2012) e46287.
[17] L.-S. Ai, et al., Gene silencing of the BDNF/TrkB axis in multiple myeloma blocks bone destruction and tumor burden in vitro and in vivo, Int. J. Cancer 133 (2013) 1074–1084.
[18] B. Choi, et al., Upregulation of brain-derived neurotrophic factor in advanced gastric cancer contributes to bone metastatic osteolysis by inducing long pentraxin 3, Oncotarget 7 (2016) 55506–55517.
[19] L.S. Weinstein, et al., Activating mutations of the stimulatory G protein in the McCune–Albright syndrome, N. Engl. J. Med. 325 (1991) 1688–1695.
[20] E. Ippolito, et al., Natural history and treatment of fibrous dysplasia of bone: a multicenter clinicopathologic study promoted by the European Pediatric Orthopaedic Society, J. Pediatr. Orthop. B 12 (2003) 155–177.
[21] T. Spencer, K.S. Pan, M.T. Collins, A.M. Boyce, The clinical Spectrum of McCune-Albright syndrome and its management, Horm. Res. Paediatr. 92 (2019) 347–356.
[22] M.H. Kelly, B. Brillante, M.T. Collins, Pain in fibrous dysplasia of bone: age-related changes and the anatomical distribution of skeletal lesions, Osteoporos. Int. 19 (2008) 57–63.
[23] T.L. Spencer, et al., Neuropathic-like pain in fibrous dysplasia/McCune-Albright syndrome, J. Clin. Endocrinol. Metab. 107 (2022) e2258–e2266.
[24] L.F. de Castro, et al., Activation of RANK/RANKL/OPG pathway is involved in the pathophysiology of fibrous dysplasia and associated with disease burden, J. Bone Miner. Res. 34 (2019) 290–294.
[25] B. Palmisano, et al., RANKL inhibition in fibrous dysplasia of bone: a preclinical study in a mouse model of the human disease, J. Bone Miner. Res. 34 (2019) 2171–2182.
[26] A. Persichetti, et al., Nanostring technology on fibrous dysplasia bone biopsies. A pilot study suggesting different histology-related molecular profiles, Bone reports 16 (2021) 101156.
[27] D. Galter, K. Unsicker, Brain-derived neurotrophic factor and trkB are essential for cAMP-mediated induction of the serotonergic neuronal phenotype, J. Neurosci. Res. 61 (2000) 295–301.
[28] I. Saggio, et al., Constitutive expression of Gsα ^{R201C} in mice produces a heritable, direct replica of human fibrous dysplasia bone pathology and demonstrates its natural history, J. Bone Miner. Res. 29 (2014) 2357–2368.
[29] E. Stack, et al., In vitro affinity optimization of an anti-BDNF monoclonal antibody translates to improved potency in targeting chronic pain states in vivo, MAbs 12 (2020).
[30] B. Palmisano, et al., GsαR201C and estrogen reveal different subsets of bone marrow adiponectin expressing osteogenic cells, Bone Res. 10 (2022) 50.
[31] B. Palmisano, M. Riminucci, G. Karsenty, Interleukin-6 signaling in osteoblasts regulates bone remodeling during exercise, Bone 176 (2023) 116870.
[32] C.A. Schneider, W.S. Rasband, K.W. Eliceiri, NIH image to ImageJ: 25 years of image analysis, Nat. Methods 9 (2012) 671–675.
[33] D.W. Dempster, et al., Standardized nomenclature, symbols, and units for bone histomorphometry: a 2012 update of the report of the ASBMR Histomorphometry Nomenclature Committee, J. Bone Miner. Res. 28 (2013) 2–17.
[34] J. Tratwal, et al., Reporting guidelines, review of methodological standards, and challenges toward harmonization in bone marrow adiposity research, Report of the Methodologies Working Group of the International Bone Marrow Adiposity Society. Front. Endocrinol. (Lausanne) 11 (2020).
[35] P. Kowiański, et al., BDNF: a key factor with multipotent impact on brain signaling and synaptic plasticity, Cell. Mol. Neurobiol. 38 (2018) 579–593.
[36] Y.-W. Su, et al., Roles of neurotrophins in skeletal tissue formation and healing, J. Cell. Physiol. 233 (2018) 2133–2145.
[37] X. Wang, J. Xu, Q. Kang, Neuromodulation of bone: role of different peptides and their interactions (review), Mol. Med. Rep. 23 (2021).
[38] N. Tomotsuka, et al., Up-regulation of brain-derived neurotrophic factor in the dorsal root ganglion of the rat bone cancer pain model, J. Pain Res. 7 (2014) 415–423.
[39] X.-H. Jin, L.-N. Wang, J.-L. Zuo, J.-P. Yang, S.-L. Liu, P2X4 receptor in the dorsal horn partially contributes to brain-derived neurotrophic factor oversecretion and toll-like receptor-4 receptor activation associated with bone cancer pain, J. Neurosci. Res. 92 (2014) 1690–1702.
[40] Y. Bao, et al., PAR2-mediated upregulation of BDNF contributes to central sensitization in bone cancer pain, Mol. Pain 10 (2014) (1744-8069-10–28).
[41] S. Kartha, M.E. Zeeman, H.A. Baig, B.B. Guarino, B.A. Winkelstein, Upregulation of BDNF and NGF in cervical intervertebral discs exposed to painful whole-body vibration, Spine (Phila. Pa. 1976) 39 (2014) 1542–1548.
[42] Y. Huang, Expression of BDNF in dorsal root ganglion of rats with bone cancer pain and its effect on pain behavior, J. Musculoskelet. Neuronal Interact. 18 (2018) 42–46.
[43] Y. Guo, et al., Integrating epigenomic elements and GWASs identifies BDNF gene affecting bone mineral density and osteoporotic fracture risk, Sci. Rep. 6 (2016) 30558.
[44] Z. Zhang, et al., BDNF regulates the expression and secretion of VEGF from osteoblasts via the TrkB/ERK1/2 signaling pathway during fracture healing, Mol. Med. Rep. 15 (2017) 1362–1367.
[45] Z. Zhang, P. Hu, Z. Wang, X. Qiu, Y. Chen, BDNF promoted osteoblast migration and fracture healing by up-regulating integrin β1 via TrkB-mediated ERK1/2 and AKT signalling, J. Cell. Mol. Med. 24 (2020) 10792–10802.
[46] V. Kauschke, et al., Effects of a pasty bone cement containing brain-derived neurotrophic factor-functionalized mesoporous bioactive glass particles on metaphyseal healing in a new murine osteoporotic fracture model, Int. J. Mol. Sci. 19 (2018).
[47] A.M. Boyce, et al., A randomized, double blind, placebo-controlled trial of alendronate treatment for fibrous dysplasia of bone, J. Clin. Endocrinol. Metab. 99 (2014) 4133–4140.
[48] B.C. Majoor, et al., Outcome of long-term bisphosphonate therapy in McCune-Albright syndrome and polyostotic fibrous dysplasia, J. Bone Miner. Res. 32 (2017) 264–276.
[49] A. Corsi, et al., Zoledronic acid in a mouse model of human fibrous dysplasia: ineffectiveness on tissue pathology, formation of “Giant osteoclasts” and Pathogenetic implications, Calcif. Tissue Int. 107 (2020) 603–610.
[50] R. Chapurlat, et al., Inhibition of IL-6 in the treatment of fibrous dysplasia of bone: the randomized double-blind placebo-controlled TOCIDYS trial, Bone 157 (2022) 116343.
[51] L.F. de Castro, et al., Safety and efficacy of Denosumab for fibrous dysplasia of bone, N. Engl. J. Med. 388 (2023) 766–768.
[52] B.C.J. Majoor, et al., Denosumab in patients with fibrous dysplasia previously treated with bisphosphonates, J. Clin. Endocrinol. Metab. 104 (2019) 6069–6078.
[53] M.E. Meier, et al., Safety of therapy with and withdrawal from denosumab in fibrous dysplasia and McCune-Albright syndrome: an observational study, J. Bone Miner. Res. 36 (2021) 1729–1738.
[54] A.M. Boyce, et al., Denosumab treatment for fibrous dysplasia, J. Bone Miner. Res. 27 (2012) 1462–1470.
[55] I. Walther, B.M. Walther, Y. Chen, I. Petersen, Analysis of GNAS1 mutations in myxoid soft tissue and bone tumors, Pathol. - Res. Pract. 210 (2014) 1–4.
[56] I. Rentería, et al., The molecular effects of BDNF synthesis on skeletal muscle: a mini-review, Front. Physiol. 13 (2022).